Cell PRESS
Immunity
Article

Guanine Nucleotide-Binding Proteins of the G_{12} Family Shape Immune Functions by Controlling $CD4^+$ T Cell Adhesiveness and Motility

Susanne Herroeder,[1,2,8] Peter Reichardt,[3] Antonia Sassmann,[1] Barbara Zimmermann,[1] Dagmar Jaeneke,[1] Jana Hoeckner,[1] Markus W. Hollmann,[4] Klaus-Dieter Fischer,[5] Stephan Vogt,[6] Robert Grosse,[1] Nancy Hogg,[7] Matthias Gunzer,[3] Stefan Offermanns,[1,9] and Nina Wettschureck[1,9,*]

[1]Institute of Pharmacology, University of Heidelberg, 69120 Heidelberg, Germany
[2]Department of Anesthesiology, University of Heidelberg, 69120 Heidelberg, Germany
[3]Institute of Molecular and Clinical Immunology, University of Magdeburg, 39120 Magdeburg, Germany
[4]Department of Anesthesiology, University of Amsterdam (AMC), 1105 DD Amsterdam, The Netherlands
[5]Institute of Biochemistry and Cell Biology and Department of Functional Genomics and Medical Toponomics, 39120 Magdeburg, Germany
[6]Department of Orthopaedic and Trauma Surgery, Technical University of Munich, 81675 Munich, Germany
[7]Leukocyte Adhesion Laboratory, Cancer Research UK, London Research Institute, WC2A 3PX London, UK
[8]Laboratory of Experimental Intensive Care & Anesthesiology (L.E.I.C.A.), Academic Medical Center Amsterdam, 1105 DD Amsterdam, The Netherlands
[9]Department of Pharmacology, Max-Planck-Institute for Heart and Lung Research, 61231 Bad Nauheim, Germany
*Correspondence: nina.wettschureck@pharma.uni-heidelberg.de
DOI 10.1016/j.immuni.2009.02.010

SUMMARY

Integrin-mediated adhesion plays a central role in T cell trafficking and activation. Genetic inactivation of the guanine nucleotide-binding (G) protein α-subunits $G\alpha_{12}$ and $G\alpha_{13}$ resulted in an increased activity of integrin leukocyte-function-antigen-1 in murine $CD4^+$ T cells. The interaction with allogeneic dendritic cells was enhanced, leading to an abnormal proliferative response in vitro. In vivo, T cell-specific inactivation of $G\alpha_{12}$ and $G\alpha_{13}$ caused lymphadenopathy due to increased lymph node entry and enhanced T cell proliferation, and the susceptibility toward T cell-mediated diseases was enhanced. Mechanistically, we show that in the absence of $G\alpha_{12}$ and $G\alpha_{13}$ the activity of the small GTPases Rac1 and Rap1 was increased, whereas signaling of the small GTPase RhoA was strongly reduced. Our data indicate that locally produced mediators signal through $G\alpha_{12}$- and $G\alpha_{13}$-coupled receptors to negatively regulate cell polarization and adhesiveness, thereby fine-tuning T cell trafficking, proliferation, and susceptibility toward T cell-mediated diseases.

INTRODUCTION

Integrin-mediated adhesion plays a central role in T cell functions. The integrin leukocyte-function-antigen-1 (LFA-1), for example, is crucial for the formation of the immunological synapse, the interface between antigen-loaded mature dendritic cells and naive T cells. LFA-1 also mediates firm adhesion to high endothelial venules, thereby allowing naive T cells to enter secondary lymphatic organs. In addition, LFA-1 has been implicated in the control of lymphocyte differentiation and proliferation, as well as in the regulation of T cell effector functions (Mor et al., 2007; Smith et al., 2007).

Given this multitude of LFA-1 functions, a precise understanding of the spatial and temporal control of the interaction between LFA-1 and its cellular counter-receptors, the intercellular adhesion molecules (ICAMs), is of great importance. In naive T cells, LFA-1 is tethered to components of the actin cytoskeleton and thereby held in the inactive state with the result that naive T cells are rounded and only mildly adhesive (Shimaoka et al., 2002; van Kooyk et al., 1999). Activation of LFA-1 occurs in response to a variety of extracellular signals, for example stimulation of cytokine receptors, the TCR-CD3 complex, or G protein-coupled receptors (GPCRs) (Kinashi, 2005). Best studied among the latter are the chemokine receptors, which have been shown to positively regulate LFA-1 through heterotrimeric G proteins of the G_i family (Laudanna and Alon, 2006; Laudanna et al., 2002). The intracellular signaling cascades mediating the effects of chemokines on integrin activation have been shown to involve several monomeric GTPases such as Rap1, Rac1, or RhoA (Mor et al., 2007). However, chemokine receptors are probably not the only GPCRs contributing to the regulation of integrin activity; T cells also express a variety of other GPCRs, such as lysophospholipid or prostanoid receptors, many of which have been implicated in the regulation of adhesiveness as well (Chun and Rosen, 2006; Matsuoka and Narumiya, 2007). In contrast to chemokine GPCRs, these receptors couple not only to G_i but also to other G protein families such as G_{12} (Riobo and Manning, 2005), but the role of this G protein family in the regulation of T cell in vivo functions has not been investigated so far.

The two members of the G_{12} family, G_{12} and G_{13}, are ubiquitously expressed and interact upon receptor-mediated activation with certain Rho guanine nucleotide exchange factors (RhoGEFs) (Fukuhara et al., 2001), which in turn mediate activation of the small GTPase RhoA. Because of the embryonic lethality of mice lacking the α-subunits of G_{12} and G_{13} ($G\alpha_{12}$ and $G\alpha_{13}$) (Gu et al., 2002; Offermanns et al., 1997), and because of the lack of specific inhibitors of these proteins, the relevance of this family in the adult organism has long been elusive. The

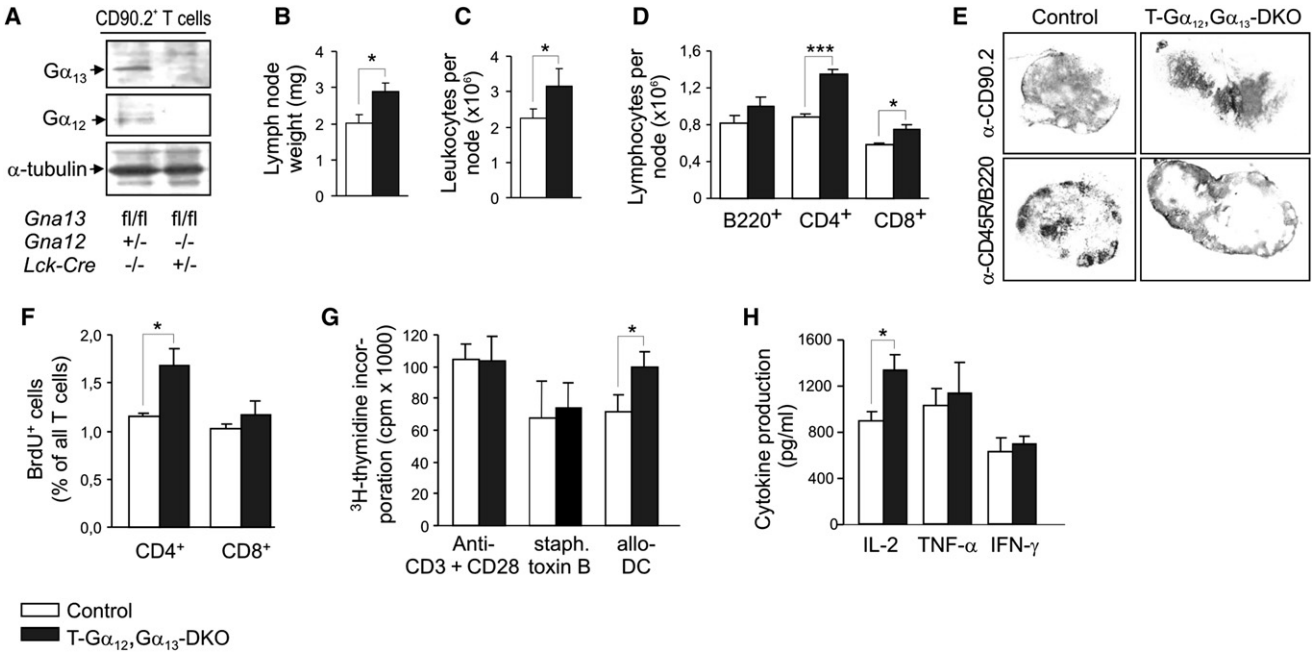

Figure 1. Lymphadenopathy in T-Gα_{12},Gα_{13} DKOs

(A) CD90.2$^+$ T cells were isolated from lymph nodes of controls (*Lck*Cre$^{-/-}$*Gna13*$^{fl/fl}$*Gna12*$^{+/-}$) and T-Gα_{12},Gα_{13} DKOs (*Lck*Cre$^{+/-}$*Gna13*$^{fl/fl}$*Gna12*$^{-/-}$) and subjected to immunoblotting with antibodies directed against Gα_{13}, Gα_{12} and α-tubulin as loading control.

(B) Weight of peripheral lymph nodes (n = 8).

(C) Leukocyte numbers per node (n = 8).

(D) Absolute numbers of CD45R/B220$^+$ B cells as well as CD4$^+$ and CD8$^+$ T cells per node (n = 10).

(E) Immunohistochemical staining of T cells and B cells in inguinal lymph nodes with antibodies against CD90.2 and CD45R/B220.

(F) Percentage of BrdU-positive T cells in lymph nodes 4 hr after intraperitoneal injection of BrdU as determined by intracellular flow cytometry (n = 6).

(G) In vitro proliferation of 2 × 10^5 CD4$^+$ T cells after 72 hr of culture with 5 × 10^4 CD11c$^+$ allo-DCs, after TCR crosslinking with immobilized CD3-CD28 antibodies, or after stimulation with staphylococcal enterotoxin B (10 ng/ml) (n = 6–10).

(H) The concentration of secreted cytokines was determined in the supernatant of cocultures between CD4$^+$ T cell and allo-DC after 72 hr (n = 8).

White bars represent the control; black bars represent the T-Gα_{12},Gα_{13} DKO. Data are displayed as mean ± SEM. *p < 0.05; ***p < 0.0005.

recent generation of tissue-specific Gα_{12},Gα_{13} double-deficient mice revealed important functions in platelets and B cells (Moers et al., 2003; Rieken et al., 2006a; Rieken et al., 2006b); the in vivo role of Gα_{12} and Gα_{13} in peripheral T cells, however, has not been addressed up to now. With the help of the Cre-loxP system, we generated T cell-specific Gα_{12},Gα_{13} double-deficient mice and show here that these proteins negatively regulate the activation state of integrin LFA-1, thereby modulating T cell trafficking and proliferation, as well as responses to foreign and self antigen.

RESULTS

Lymphadenopathy in T Cell-Specific Gα_{12},Gα_{13} Double-Deficient Mice

T cell-specific Gα_{12},Gα_{13} double-deficient mice were generated by intercrossing animals in which the gene coding for Gα_{13}, *Gna13*, was flanked by loxP sites (*Gna13*$^{fl/fl}$) with the T cell-specific *Lck*-Cre line (*Lck*Cre$^{+/-}$) and constitutively Gα_{12}-deficient (*Gna12*$^{-/-}$) mice (Gu et al., 2002; Hennet et al., 1995; Moers et al., 2003). As controls we used *Lck*Cre$^{-/-}$*Gna13*$^{fl/fl}$*Gna12*$^{+/-}$ littermates throughout the study. Immunoblots showed that Gα_{13} immunoreactivity was strongly reduced and that Gα_{12} was absent in extracts of isolated CD90.2$^+$ (Thy1.2) T cells (Figure 1A). T cell-specific Gα_{12},Gα_{13} double-deficient mice were born at expected frequencies and were viable and fertile, but showed an increased size and weight of axillary, cervical, and inguinal lymph nodes (Figure 1B). Mesenteric lymph nodes were enlarged as well, whereas Peyer's patches appeared normal (data not shown). The increased lymph node weight corresponded to increased cell numbers (Figure 1C), and flow cytometric analysis of lymphocyte subpopulations revealed that this was predominantly a result of an expansion of the CD4$^+$ T cell population (Figure 1D). The general organization into B cell follicles and T cell areas was not disturbed (Figure 1E). The relative numbers of CD4$^+$ regulatory T cells and CD4$^+$ memory-effector T cells within lymph nodes were not altered (data not shown). In addition to lymphadenopathy, T cell-specific Gα_{12},Gα_{13} double-deficient mice showed an increased thymic weight and cell number, with a proportionate increase in all subpopulations (Table S1 available online). There were no substantial differences with respect to the expression of TCRβ chain, CD3ε, CD69, or CD5 in the different thymic subpopulations (data not shown). The splenic weight and splenocyte numbers were increased, although not significantly (p = 0.08 and 0.27, respectively). The CD4$^+$ T cell population in the blood was increased (Table S1). Taken together, these results show that genetic inactivation of Gα_{12} and Gα_{13} in T cells resulted in an increased cell number especially of CD4$^+$ T cells in lymph nodes, blood, and the

thymus, suggesting that these G proteins have regulatory functions in $CD4^+$ T cell proliferation, apoptosis, or trafficking.

Proliferation Is Enhanced in $G\alpha_{12},G\alpha_{13}$ Double-Deficient $CD4^+$ T Cells

To study the causes of lymphadenopathy in T cell-specific $G\alpha_{12},G\alpha_{13}$ double-deficient mice, we investigated apoptosis and proliferation. Apoptosis, here determined as the percentage of Annexin V-positive T cells in freshly isolated lymph nodes, did not differ between the genotypes (data not shown). To assess basal T cell proliferation in lymph nodes, we determined the percentage of 5-bromo-2-deoxyuridine (BrdU) incorporating T cells 4 hr after intraperitoneal injection of BrdU. We found that lymph nodes from mutant mice contained more BrdU-positive $CD4^+$ T cells than those from control animals, whereas the proportion of BrdU-positive $CD8^+$ T cells was not increased (Figure 1F). We next determined in vitro proliferation by measuring the incorporation of [^{3}H]-thymidine into $CD4^+$ T cells after 72 hr of culture. Although there was no difference in the proliferation of unstimulated $CD4^+$ T cells, mutant cells showed an increased proliferation in response to allogeneic splenic $CD11c^+$ dendritic cells (allo-DCs) (Figure 1G). In contrast, the proliferative response induced by CD3-CD28 crosslinking, staphylococcal enterotoxin B, or phorbol-12-myristate-13-acetate (PMA) did not differ between the genotypes (Figure 1G and data not shown).

To test whether increased proliferation in response to allo-DCs was accompanied by altered cytokine production, we determined cytokine amounts in the supernatant of cocultures between $CD4^+$ T cell and allo-DCs by ELISA. The production of interleukin (IL)-2 was increased in mutant cells, whereas the production of tumor necrosis factor-α (TNFα) or interferon-γ (IFNγ) remained unchanged (Figure 1H). Taken together, these results indicate that $G\alpha_{12}$ and $G\alpha_{13}$ negatively regulate $CD4^+$ T cell proliferation in response to allogeneic dendritic cells.

$G\alpha_{12},G\alpha_{13}$ Double-Deficient $CD4^+$ T Cells Show Enhanced Interaction with Dendritic Cells

Because the G_{12} family is known to contribute to the regulation of cellular adhesiveness, we investigated whether the enhanced proliferation in response to allo-DCs was due to abnormal cell-cell interactions in mutant cells. Flow cytometric analysis of conjugate formation between fluorescently labeled $CD4^+$ T cells and allo-DCs revealed an increased interaction if the $CD4^+$ T cells were $G\alpha_{12},G\alpha_{13}$ deficient (Figure 2A). We next investigated the interaction between purified $CD4^+$ T cells and fluorescently labeled allo-DCs by live-cell imaging (Figure 2B and Movies S1 and S2). In mutant $CD4^+$ T cells, the proportion of cells with stable DC interactions (“stable” here defined as an interaction that lasted throughout a 10 min movie) was increased (Figure 2C and Movies S1 and S2), as well as the interaction between $CD4^+$ T cells themselves (Figure 2D). These data suggest an important role of $G\alpha_{12}$ and $G\alpha_{13}$ in the regulation of cellular interactions between $CD4^+$ T cells and allo-DCs.

LFA-1 Activity Is Increased in $G\alpha_{12},G\alpha_{13}$ Double-Deficient $CD4^+$ T Cells

To further investigate LFA-1 activity in mutant cells, we compared adhesiveness of control and $G\alpha_{12},G\alpha_{13}$ double-deficient $CD4^+$ T cells on ICAM-1- and VCAM-1 (vascular cell

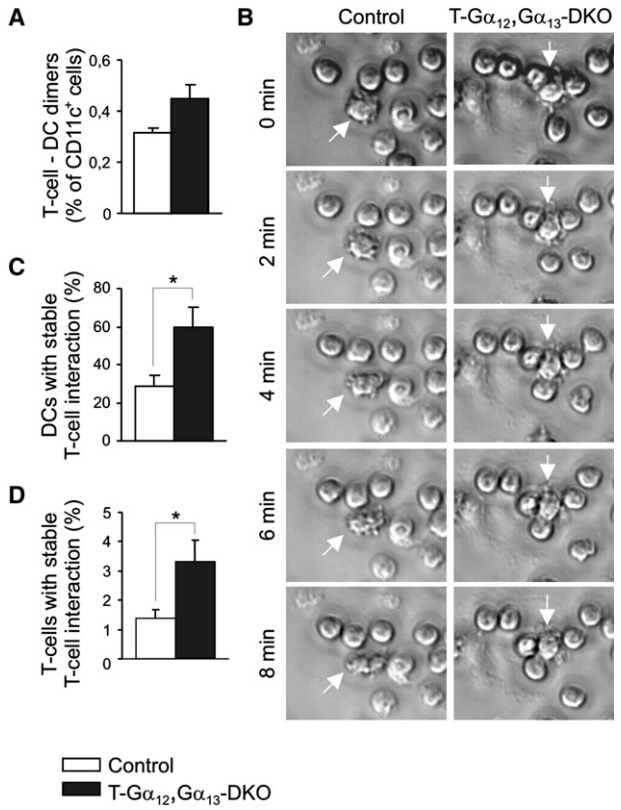

Figure 2. Cell-Cell Interactions of $G\alpha_{12},G\alpha_{13}$ double-deficient $CD4^+$ T Cells

(A) Flow cytometric analysis of dimer formation between CD4-PE-labeled T cells and CD11c-FITC-labeled allo-DCs (n = 8).

(B) Live-cell imaging of isolated $CD4^+$ T cells and CFSE-labeled allo-DCs. Time-lapse movies of 10 min duration were recorded and exemplary micrographs are depicted (magnification 40×). The microphotographs taken at 0 min are overlaid with the GFP fluorescence image for identification of CFSE-labeled DCs (marked by white arrows).

(C and D) Statistical evaluation of stable interactions between $CD4^+$ T cells and DCs (C) or between $CD4^+$ T cells (D).

White bars represent the control; black bars represent the T-$G\alpha_{12},G\alpha_{13}$ DKO. Data are displayed as mean ± SEM. *$p < 0.05$.

adhesion molecule-1)-coated plastic (Figure 3A). On ICAM-1, mutant cells showed a higher basal adhesion than control cells, whereas there was no difference with respect to basal adhesion on VCAM-1. Mutant cells also showed increased ICAM-1 adhesiveness after integrin activation by chemokines or Mg^{2+} and EGTA, whereas no differences were found in response to PMA or TCR crosslinking (data not shown). On VCAM-1, none of these integrin activators resulted in a substantial difference between the genotypes (Figure 3A and data not shown).

LFA-1 activation has been shown to involve two modalities, increased affinity and enhanced integrin clustering (Hogg et al., 2002; Laudanna et al., 2002). To assess LFA-1 affinity, we determined binding of soluble ICAM-1 to $CD4^+$ T cells in a flow cytometric assay and found that in mutant T cells, the proportion of cells that bound ICAM-1 was increased both under basal conditions and after stimulation with Mg^{2+} and EGTA, which are known to increase LFA-1 affinity (Figure 3B). We next investigated LFA-1 clustering by immunofluorescent staining of the

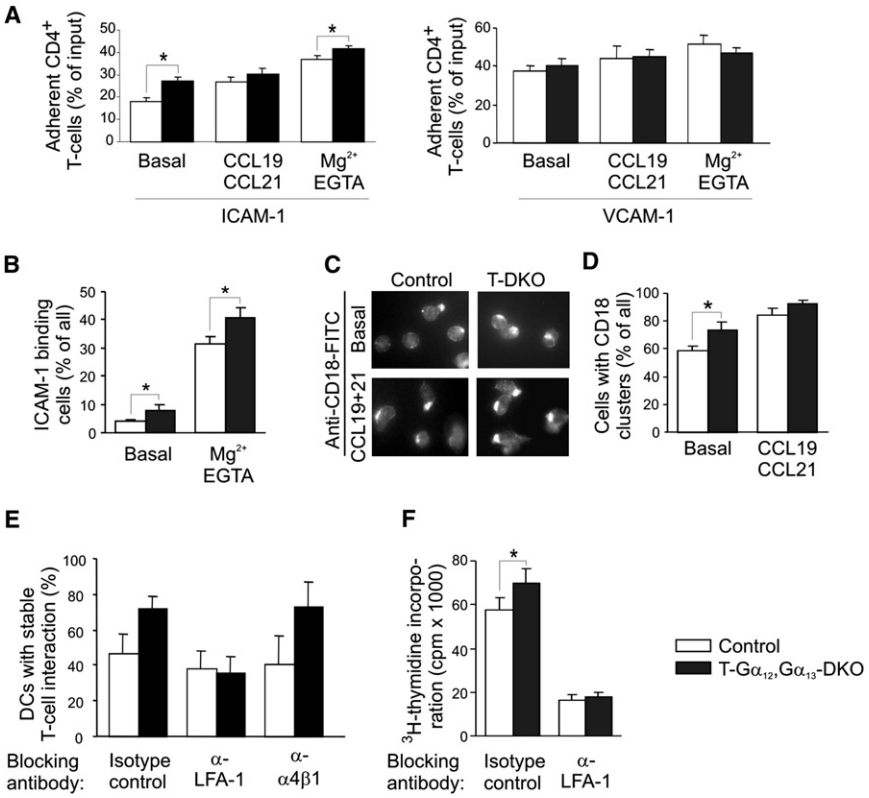

Figure 3. LFA-1 Activity in $G\alpha_{12}$,$G\alpha_{13}$ double-deficient $CD4^+$ T Cells

(A) Adhesion of lymph node $CD4^+$ T cells to ICAM-1- or VCAM-1-coated plastic. The percentage of adherent $CD4^+$ T cells was determined by flow cytometry after 30 min of incubation under basal conditions as well as after stimulation with chemokines CCL19 and 21 (CCL19+21) or Mg^{2+}+EGTA. Data are expressed as percent of input (n = 8).

(B) Flow cytometric analysis of basal and Mg^{2+}+EGTA-induced binding of fluorescently labeled soluble ICAM-1 to $CD4^+$ T cells (n = 6).

(C and D) Basal and CCL19+21-induced LFA-1 clustering in $CD4^+$ T cells was determined by immunofluorescent staining with an CD18 antibody. (C) shows exemplary photomicrographs of CD18-stained cells (magnification 63×). (D) shows statistical evaluation of the percentage of cells showing CD18 clusters (n = 3).

(E) Effect of blocking antibodies directed against LFA-1, α4β1, or isotype control on T cell-DC interactions in live-cell imaging (n = 3).

(F) Effect of blocking antibodies directed against LFA-1 on $CD4^+$ T cell proliferation in response to DCs (n = 6).

White bars represent the control; black bars represent the T-$G\alpha_{12}$,$G\alpha_{13}$ DKO. Data are displayed as mean ± SEM. *$p < 0.05$.

LFA-1 β-chain CD18 and found that the proportion of cells with clusters was increased in mutant $CD4^+$ T cells under basal conditions and, less prominently, after chemokine stimulation (Figures 3C and 3D). However, because LFA-1 clustering was shown to follow ligand binding (Kim et al., 2004), these findings might represent a direct consequence of increased affinity. To exclude that the observed differences were due to an increased surface expression of LFA-1, we analyzed expression of the α- and β-chains of LFA-1 by flow cytometry, but found no abnormalities (data not shown). In order to test whether increased LFA-1 activity in $G\alpha_{12}$,$G\alpha_{13}$ double-deficient $CD4^+$ T cells altered integrin outside-in signaling, we studied phosphorylation of extracellular signal-regulated kinase (ERK) in response to Mn^{2+} and integrin crosslinking, but failed to detect differences between the genotypes. Also, ERK phosphorylation in response to TCR crosslinking or PMA was not altered (Figure S1).

To test whether increased interactions between mutant T cells and allo-DCs were indeed due to increased LFA-1 activity, we performed live-cell imaging in the presence of blocking antibodies directed against LFA-1. Whereas LFA-1 antibodies had only a minor effect on control $CD4^+$ T cells, they normalized enhanced interactions of $G\alpha_{12}$,$G\alpha_{13}$ double-deficient $CD4^+$ T cells. In contrast, α4β1 antibodies had no effect on either control or mutant cells (Figure 3E). To further test whether increased LFA-1 activity also contributed to enhanced proliferation of $G\alpha_{12}$,$G\alpha_{13}$ double-deficient $CD4^+$ T cells, we performed in vitro proliferation assays with allo-DCs in the presence of blocking antibodies directed against LFA-1. This treatment reduced proliferation in mutant cells to the degree found in control cells (Figure 3F), suggesting that deregulation of LFA-1 activity importantly contributes to hyperproliferation of mutant T cells. Taken together, these findings indicate that inactivation of $G\alpha_{12}$ and $G\alpha_{13}$ results in $CD4^+$ T cells in an increased affinity and avidity of LFA-1, which in turn leads to an increased interaction with antigen-presenting cells.

Polarization and Migration in the Absence of $G\alpha_{12}$ and $G\alpha_{13}$

In addition to increased LFA-1 avidity and affinity, morphological changes such as increased spreading might contribute to increased adhesiveness in the absence of $G\alpha_{12}$ and $G\alpha_{13}$. To investigate cell shape in vitro, we performed phalloidin stainings of polymerized actin in ICAM-1 adherent $CD4^+$ T cells. We found that the proportion of cells with firmly attached rear end and elongated tail was substantially increased in mutant cells (Figures 4A and 4B), as was the percentage of polarized cells (Figure 4C). To correlate these morphological changes with potential changes in migratory behavior, we performed time-lapse video microscopy of $CD4^+$ T cells on ICAM-1-coated plastic. The distance traveled by individual $CD4^+$ T cells was decreased in the absence of $G\alpha_{12}$,$G\alpha_{13}$ (Figure 4D and Movies S3 and S4), whereas the proportion of motile cells did not differ between the genotypes (Figure 4E). We next investigated whether increased adhesiveness and polarization would affect transmigration through transwell inserts coated with ICAM-1 or bEND.3 endothelial cells. Under basal conditions, mutant cells showed reduced transmigration both through ICAM-1 and endothelial cells, although migration in response to chemokines CCL19 and CCL21 was not impaired (Figure 4F).

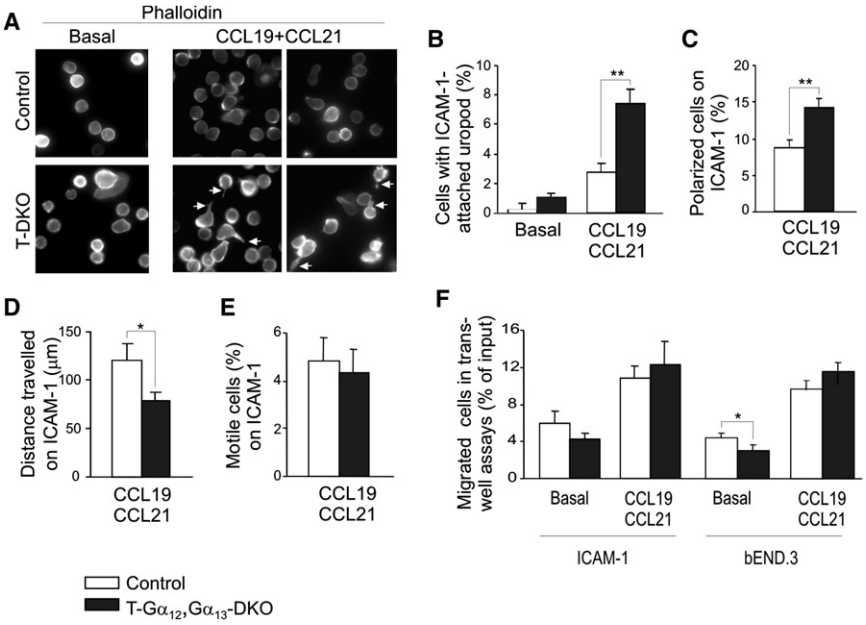

Figure 4. Migratory Behavior of Mutant CD4⁺ T Cells

(A) Exemplary photomicrographs taken from phalloidin-stained CD4⁺ T cells that have adhered for 20 min to ICAM-1-coated plastic in the absence (basal) or presence of CCL19+21 (magnification 63×).

(B) Statistical analysis of the percentage of cells with attached, elongated rear (n = 3).

(C) Percentage of CD4⁺ T cells with a polarized phenotype (showing one or more F-actin positive pseudopods) (n = 3).

(D) The distance traveled by CCL19+21-stimulated CD4⁺ T cells was determined on ICAM-1-coated plastic in time-lapse microscopy.

(E) Percentage of motile CD4⁺ T cells (i.e., traveling more than one body length per 10 min) (n = 3).

(F) Percentage of CD4⁺ T cells that have migrated through ICAM-1-coated transwells inserts (left) or inserts covered with a confluent monolayer of bEND.3 endothelial cells (right) during 3 hr of incubation without agonist in the lower chamber (basal) or in response to CCL19+21 (n = 5).

White bars represent the control; black bars represent the T-$G\alpha_{12}$,$G\alpha_{13}$ DKO. Data are displayed as mean ± SEM. *$p < 0.05$; **$p < 0.005$.

Enhanced Lymph Node Entry of Deficient CD4⁺ T Cells

In addition to increased proliferation, LFA-1 hyperactivity in the absence of $G\alpha_{12}$ and $G\alpha_{13}$ might affect T cell trafficking into lymph nodes, thereby contributing to lymphadenopathy. To study whether increased adhesiveness to ICAM-1 altered T cell trafficking in vivo, we performed adoptive transfer experiments with fluorescently labeled purified CD4⁺ T cells from control and mutant mice. Twenty-four hours after injection, significantly more mutant than control cells were found in cervical lymph nodes of the respective host (Figure 5A). Because this might be a result of altered entry and/or exit, we repeated these experiments at 2 hr after transfer and found that even at this time point, mutant CD4⁺ T cells were overrepresented (Figure 5B). Also the entry of deficient CD4⁺ T cells into the spleen was increased at two hours after transfer, whereas numbers of mutant cells in the blood were reduced (Figure 5B). Intravenous injection of LFA-1 antibodies into hosts 30 min prior to adoptive transfer normalized the increased entry of $G\alpha_{12}$,$G\alpha_{13}$ double-deficient CD4⁺ T cells (Figure 5C), suggesting that increased LFA-1 activity, but not disinhibition of other integrins such as $\alpha4\beta1$, underlies enhanced entry.

To investigate in vivo whether increased adhesiveness of $G\alpha_{12}$,$G\alpha_{13}$ double-deficient CD4⁺ T cells leads to a logjam of cells within the lymphatic vessels or to the opposite, a more efficient transendothelial migration, we performed two-photon intravital microscopy of inguinal lymph nodes 2 hr after adoptive transfer (Figures 5D and 5E). We determined the numbers of control and $G\alpha_{12}$,$G\alpha_{13}$ double-deficient CD4⁺ T cells in (1) a vessel-rich zone, comprising mostly medulla, containing higher-order venules and high endothelial venules (HEV), and in (2) the T cell zone itself. Two hours after transfer, neither control nor mutant CD4⁺ T cells were detected directly attached to HEV endothelium; all cells had transmigrated through the venule wall. Within the lymphatic tissue, the majority of cells had already proceeded to dense lymphatic tissues, i.e., to the proper T cell zones. A minority of CD4⁺ T cells was found in the vessel rich zone, where $G\alpha_{12}$,$G\alpha_{13}$ double-deficient cells were overrepresented (Figure 5E). These findings indicate that enhanced transendothelial migration without persistent attachment to HEV is the main factor underlying the observed dominance of $G\alpha_{12}$,$G\alpha_{13}$ double-deficient CD4⁺ T cells in the lymph node 2 hr after adoptive transfer.

To also address the question of potentially impaired lymph node egress, we studied transwell migration of $G\alpha_{12}$,$G\alpha_{13}$ double-deficient CD4⁺ T cells in response to the GPCR agonist sphingosine 1-phosphate (S1P), which has been shown to regulate egress from lymph node or thymus through the $S1P_1$ receptor (Matloubian et al., 2004). However, neither with ICAM-1-coated nor with uncoated transwell inserts did we observe differences between the genotypes with respect to S1P-induced migration (Figure 5F and data not shown), and such a finding is in line with the assumption that $S1P_1$ is a predominantly G_i-coupled receptor (Chun and Rosen, 2006). To address the possibility of an egress impairment independent of S1P, we analyzed the percentage of dye-positive cells 24 hr after adoptive transfer in the cisterna chyli, which collects efferent lymph from the lower body. Also in cisterna chili lymph, mutant CD4⁺ T cells were overrepresented, suggesting that the passage time through lymph nodes was not altered (Figure 5G). In summary, these results show that increased LFA-1-mediated adhesion in $G\alpha_{12}$,$G\alpha_{13}$ double-deficient CD4⁺ T cells does not only result in an enhanced interaction with allo-DCs but also facilitates entry into lymph nodes.

Signaling Pathways Involved in $G\alpha_{12}$,$G\alpha_{13}$-Mediated Regulation of LFA-1

We next attempted to elucidate the molecular mechanisms underlying increased integrin activation and polarization in $G\alpha_{12}$,$G\alpha_{13}$ double-deficient CD4⁺ T cells. Small GTPases such as Rap1, RhoA, and Rac1 are known to regulate integrin activity

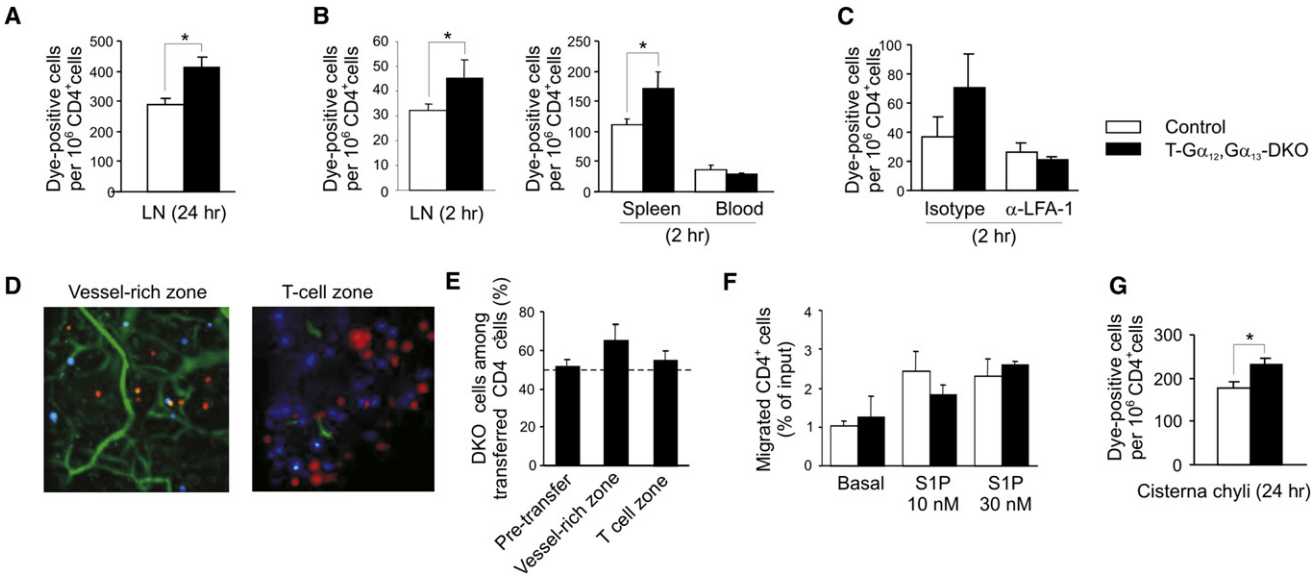

Figure 5. Lymph Node Homing In Vivo

(A–C) Differentially labeled $CD4^+$ T cells from control and mutant mice were mixed in a 1:1 ratio and injected intravenously into wild-type recipients (5×10^6 per mouse). After 24 (A) or 2 (B) hr, the proportion of labeled $CD4^+$ T cells was determined by flow cytometry (data are corrected for actual input ratio as determined by FACS). At 2 hr, spleen and blood were also investigated (n = 6–8). (C) shows the adoptive transfer into wild-type recipients pretreated with blocking LFA-1 antibodies or isotype control (n = 4).

(D and E) Intravital two-photon microscopy was used for analyzing the distribution of control versus $G\alpha_{12},G\alpha_{13}$ double-deficient $CD4^+$ T cells in the inguinal lymph node 2 hr after adoptive transfer. (D) shows examples for the different areas studied (control cells in red, mutant cells in blue). (E) shows the statistical evaluation of the percentage $G\alpha_{12},G\alpha_{13}$ double-deficient $CD4^+$ T cells found in the two respective image zones and in FACS analysis of the transferred population (n = 3).

(F) Migration of control and mutant $CD4^+$ T cells through uncoated transwell inserts in response to S1P.

(G) Proportion of dye-positive cells in cisterna chyli aspirates 24 hr after adoptive transfer.

White bars represent the control; black bars represent the T-$G\alpha_{12},G\alpha_{13}$ DKO. Data are displayed as mean ± SEM. *$p < 0.05$.

and cell polarization in response to chemokines (Iden and Collard, 2008; Laudanna and Alon, 2006; Mor et al., 2007); we therefore studied the activation state of these signaling molecules in the absence of $G\alpha_{12}$ and $G\alpha_{13}$ (Figure 6). Both in control and $G\alpha_{12},G\alpha_{13}$ double-deficient cells, active Rap1 was barely detectable in the basal state, but strongly increased 20 and 60 s after application of CCL19 and CCL21, and this increase was even more prominent in $G\alpha_{12},G\alpha_{13}$ double-deficient cells (Figure 6A).

Although the potential interactions between the G_{12} family and Rap1 still need to be elucidated, the small GTPase RhoA is a well-known effector of G_{12} and G_{13}. We studied RhoA activation in response to stimulation of known G_{12},G_{13}-coupled receptors such as the TXA_2 receptor TP (Matsuoka and Narumiya, 2007) or LPA receptors (Chun and Rosen, 2006) and found that the TP agonist U46619, as well as LPA, induced a robust RhoA activation in control $CD4^+$ T cells, but not in $G\alpha_{12},G\alpha_{13}$ double-deficient $CD4^+$ T cells (Figure 6B). Interestingly, also basal RhoA activity was reduced in $G\alpha_{12},G\alpha_{13}$ double-deficient cells. Given that RhoA has been shown to negatively regulate Rac1 (Iden and Collard, 2008), we next studied basal and chemokine-induced Rac1 activation. We found that Rac1 activation was generally enhanced in mutant cells, most prominently at 60 s after stimulation, but also under basal conditions (Figure 6C). The G_{12},G_{13}-mediated signaling pathway obviously exerts an inhibitory effect on chemokine-induced Rac1 activation, and two different scenarios might underlie this finding: (1) CCR7 directly activates G_{12} and G_{13} in parallel with its main effector pathway G_i, or (2) the CCR7-G_i-Rac1 signaling cascade is modulated by other receptors than CCR7. To address the first possibility, we investigated whether CCL19 and CCL21 were able to induce RhoA activation in T cells and whether this depended on G_i and/or on G_{12} and G_{13} (Figure 6D). We found that CCL19+21 induced a mild RhoA activation in control T cells, but the response was weaker and slower than that induced by the TXA_2 analog U46619. Pretreatment with pertussis toxin, which ADP-ribosylates G_i and thereby uncouples it from receptors, did not affect U46619-induced RhoA activation but abrogated chemokine-induced RhoA activation. In $G\alpha_{12},G\alpha_{13}$ double-deficient T cells, U46619-induced RhoA activation was clearly reduced, whereas RhoA activation in response to CCL19+21 was not changed compared to control cells (Figure 6D). These findings indicate that the mild RhoA activation observed after CCR7 stimulation is rather mediated through G proteins of the G_i family than the G_{12} family.

To investigate the potential involvement of other GPCRs in this context, we tested whether concomitant activation of the G_{12},G_{13}-RhoA pathway, for example in response to U46619, was able to quench chemokine-induced Rac1 activation in wild-type cells. We found that coapplication of U46619 with chemokines induced a strong RhoA activation within 20 s (Figure 6E) and that Rac1 activation was concomitantly reduced (Figure 6F). Of note, the quenching effect of U46619 on chemokine-induced Rac1 activation was abrogated in $G\alpha_{12},G\alpha_{13}$ double-deficient

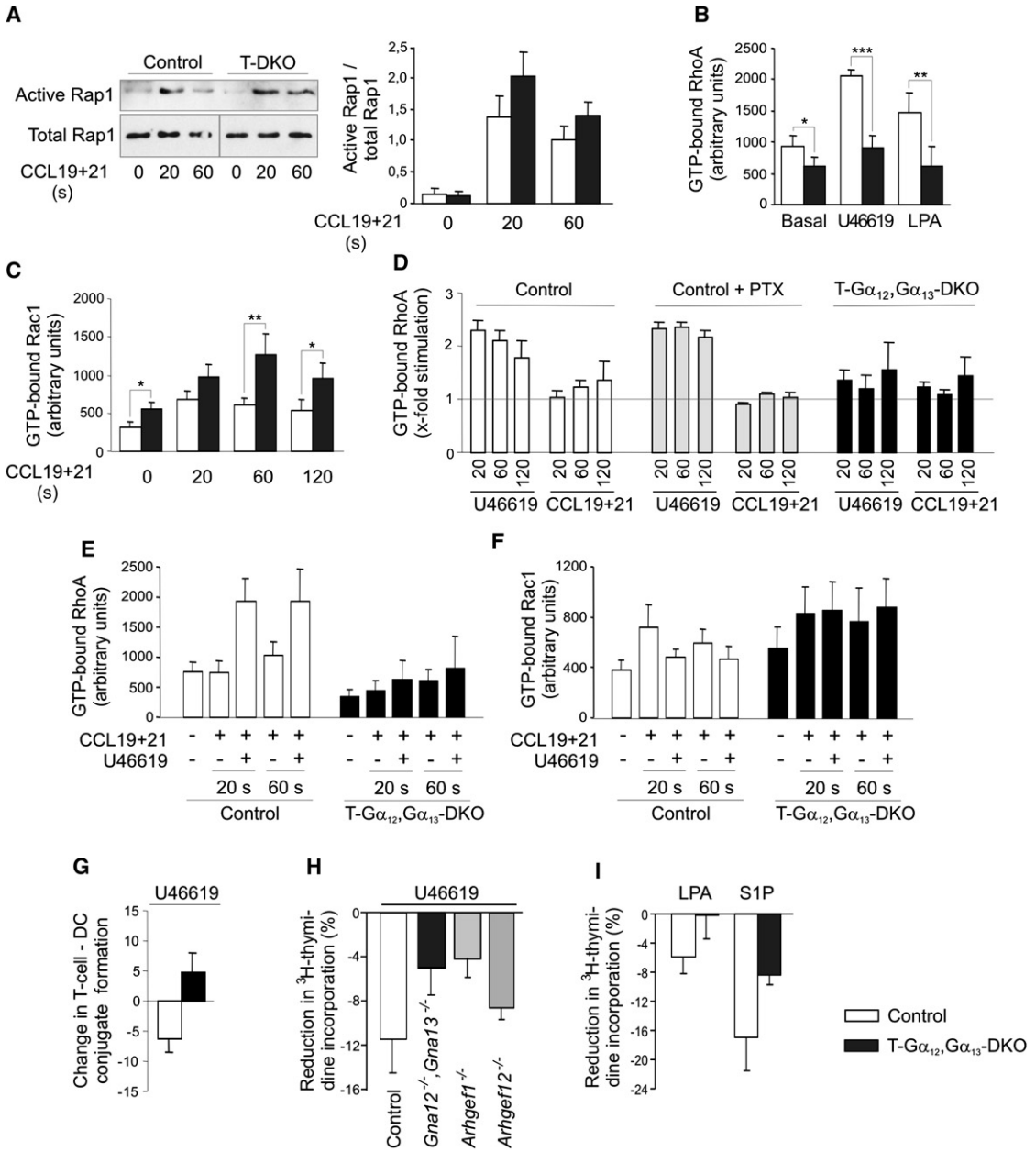

Figure 6. Signaling Pathways Involved in $G\alpha_{12},G\alpha_{13}$-Mediated Regulation of Adhesiveness and Polarization

(A) Basal and CCL19+21-induced Rap1 activation in control and $G\alpha_{12},G\alpha_{13}$ double-deficient T cells. The left panel shows exemplary immunoblots. The right panel shows the statistical evaluation of the densitometric quantification (n = 5).

(B) Amounts of active, GTP-bound RhoA under basal conditions and 1 min after stimulation with the TXA_2 analog U46619 or lysophosphatidic acid (LPA) (n = 6–10).

(C) Basal and CCL19+21-induced Rac1 activation in $CD4^+$ T cells (n = 6–10).

(D) Comparison of relative RhoA activation in response to U46619 and CCL19+21 in control T cells, pertussis toxin (PTX)-pretreated T cells, and $G\alpha_{12},G\alpha_{13}$ double-deficient T cells (n = 3).

(E and F) Effect of U46619 on CCL19+21-induced activation of RhoA (E) and Rac1 (F) (n = 4–6).

(G) Effect of U46619 on conjugate formation between control or mutant $CD4^+$ T cells and allo-DCs as determined by flow cytometry (n = 5).

(H) Effect of U46619 on allo-$CD11c^+$-induced proliferation in control $CD4^+$ T cells, as well as $CD4^+$ T cells deficient for $G\alpha_{12},G\alpha_{13}$ (*Gna12*$^{-/-}$,*Gna13*$^{-/-}$), Lsc (*Arhgef1*$^{-/-}$), or LARG (*Arhgef12*$^{-/-}$) (n = 3–5).

(I) Effect of LPA and S1P on allo-$CD11c^+$-induced proliferation in control and $G\alpha_{12},G\alpha_{13}$ double-deficient $CD4^+$ T cells (n = 3–5).

White bars represent the control; black bars represent the T-$G\alpha_{12},G\alpha_{13}$ DKO. s, seconds. Data are displayed as mean ± SEM. *$p < 0.05$.

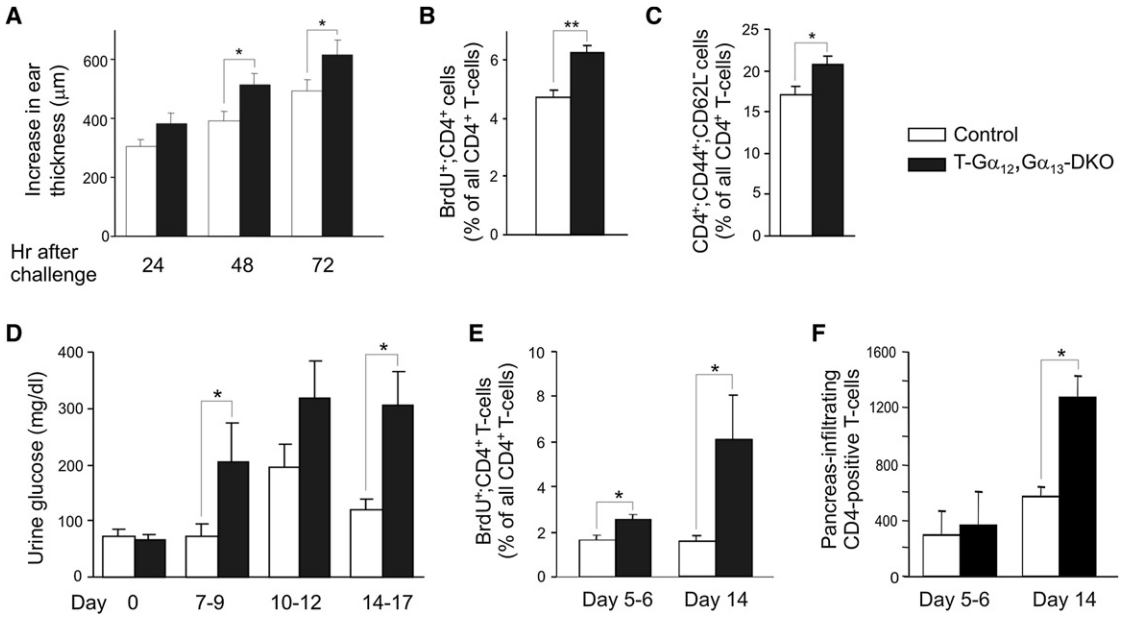

Figure 7. Immune Responses in T-G$\alpha_{12/13}$ DKOs

(A–C) Delayed type hypersensitivity. (A) shows an increase in ear thickness after sensitization and challenge with DNFB (n = 10). (B) and (C) show flow cytometric analysis of BrdU-positive $CD4^+$ T cells (B) and of $CD4^+$,$CD44^+$,$CD62L^-$ effector and memory T cells (C) in cervical lymph nodes 72 hr after challenge (n = 6). (D–F) MLD-STZ-induced diabetes mellitus. (D) shows urine glucose amounts at different time points after disease induction (n = 10). (E) shows flow cytometric analysis of BrdU-positive $CD4^+$ T cells in peripancreatic lymph nodes before onset of symptoms (days 5–6) and in the late phase of disease (day 14) (n = 4). (F) shows flow cytometric analysis of pancreatic infiltrates at days 5–6 and day 14 (n = 4–6). White bars represent the control; black bars represent the T-Gα_{12},Gα_{13} DKO. Data are displayed as mean ± SEM. *$p < 0.05$.

cells (Figure 6F), in which RhoA activation was strongly reduced (Figure 6E).

We next asked whether U46619-induced activation of the G_{12},G_{13}-RhoA-signaling cascade would also affect cell-cell interactions and, secondary to that, proliferation. We found that U46619 reduced dimer formation between control $CD4^+$ T cells and allo-DCs, whereas it moderately increased conjugate formation in Gα_{12},Gα_{13} double-deficient $CD4^+$ T cells (Figure 6G). Furthermore, U46619 reduced in vitro proliferation of control $CD4^+$ T cells, and this effect was impaired in mutant cells (Figure 6H). We next investigated the potential involvement of the G_{12},G_{13}-regulated RhoGEF proteins Lsc-p115RhoGEF (Lsc) and leukemia-associated RhoGEF (LARG) in this process and found that U46619-induced suppression of proliferation was reduced in Lsc-deficient cells as well (Figure 6H). Also, inactivation of LARG led to some reduction, although a less prominent one, suggesting that both LARG and Lsc contribute to the effects of Gα_{12},Gα_{13} on adhesiveness and proliferation, with a predominant role of Lsc (Figure 6H). Interestingly, lysophospholipids LPA and S1P also were able to reduce proliferation in response to allo-DCs in a Gα_{12},Gα_{13}-dependent manner (Figure 6I). Of note, the inhibitory effects of U46619, LPA, and S1P on proliferation are mild compared to the effect of LFA-blocking antibodies, showing that the G_{12},G_{13}-mediated signaling pathway only exerts a modulating role. Taken together, these results suggest that GPCRs such as the TXA_2 receptor, but also LPA and S1P receptor subtypes, negatively regulate cell adhesion and polarization through G_{12},G_{13}-mediated activation of RhoA, which in turn modulates chemokine-induced activation of Rac1, and, directly or indirectly, Rap1 (Figure S2). We hypothesize that TXA_2 or LPA regulate adhesiveness of $CD4^+$ T cells in an auto- or paracrine manner; in support of this hypothesis, we found that gentle washing of cells enhanced ICAM-1 adhesion, but not VCAM-1 adhesion (Figure S3).

Immune Functions In Vivo

Increased $CD4^+$ T cell proliferation and trafficking might alter responses to exogenous or endogenous antigens, resulting in abnormal immune responses or autoimmune disease. Neither routine histological analysis of internal organs nor staining for IgG deposition in the kidney of aged mice revealed signs of spontaneous autoimmune disease (data not shown), which led us to challenge T cell-specific Gα_{12},Gα_{13} double-deficient mice in two models of T cell-mediated pathology: contact hypersensitivity to dinitrofluorobenzene (DNFB) as a model for responses to foreign antigen (Kurimoto and Streilein, 1993) and low-dose streptozotocin-induced diabetes mellitus as a model of autoimmune disease (Like and Rossini, 1976).

During the sensitization phase of contact hypersensitivity, the hapten DNFB is applied to the abdominal skin from where it is transported to draining lymph nodes and presented by dendritic cells. The resulting activation of naive T cells and generation of effector cells leads during the elicitation phase (rechallenge with DNFB in the ear of the skin) to leukocyte recruitment to the ear, resulting in a Th1-cell-dependent local inflammation with consecutive swelling (Kurimoto and Streilein, 1993). We found that T cell-specific Gα_{12},Gα_{13} double-deficient mice showed increased ear swelling at 24, 48, and 72 hr after sensitization and challenge (Figure 7A), and histological analyses of ear

sections taken at 72 hr showed an increased leukocytic infiltration (data not shown). Basal ear thickness and histology did not differ between the genotypes (data not shown). $CD4^+$ T cells in cervical lymph nodes from mutant mice showed a higher proliferation rate than those of control mice (Figure 7B), and the proportion of T memory and effector cells was increased (Figure 7C).

In the second in vivo model, type I diabetes mellitus is induced by intraperitoneal administration of multiple low doses of streptozotocin (MLD-STZ), and the pathogenesis of this disease has been shown to involve an autoimmune-mediated destruction of pancreatic β-cells (Like and Rossini, 1976). We determined urine glucose levels every 72–96 hr starting from the seventh day after diabetes induction and found that in deficient mice diabetes development was both accelerated and aggravated (Figure 7D). Because this might be due to an increased proliferative response to an altered cytokine profile, or to increased entry into inflamed tissues, we investigated proliferation, cytokine production and number of infiltrating leukocytes before onset of symptoms (days 5–6) and at the height of disease (day 14). We found that peripancreatic lymph nodes were clearly enlarged already at day 5–6 (total cell number control mice: $9.8 \pm 3.4 \times 10^6$, mutant mice: $25.9 \pm 5.8 \times 10^6$); the $CD4^+$ T cells showed enhanced proliferation (Figure 7E) without substantial changes in the production of IFNγ, TNFα, or IL-4 (data not shown). The numbers of pancreas-infiltrating $CD4^+$ T cells, $CD8^+$ T cells, or $CD11b^+$ macrophages did not differ between the genotypes at days 5–6; at day 14, however, T cell-specific $G\alpha_{12}$,$G\alpha_{13}$ double-deficient mice showed increased numbers of pancreas-infiltrating $CD4^+$ T cells (Figure 7F and data not shown). Taken together, these findings show that the enhanced proliferative responses in T cell-specific $G\alpha_{12}$,$G\alpha_{13}$ double-deficient mice are associated with an increased susceptibility and severity of T cell-mediated diseases.

DISCUSSION

Whereas G_i-coupled chemokine receptors have in many studies been shown to importantly contribute to T cell trafficking or formation of the immunological synapse (Kinashi, 2005; Laudanna et al., 2002), the role of the G_{12} family in peripheral T cells is poorly understood. We report here that $G\alpha_{12}$,$G\alpha_{13}$ double-deficient $CD4^+$ T cells show an enhanced interaction with allo-DCs, thereby leading to abnormal proliferative responses in vitro. Together with an increased lymph node entry, this enhancement of proliferation most likely underlies the increased lymph node size observed in T cell-specific $G\alpha_{12}$,$G\alpha_{13}$ double-deficient mice in vivo. Our in vitro studies suggest an increased activity of integrin LFA-1 as an underlying mechanism, and this notion is strongly supported by the finding that blocking antibodies directed against LFA-1 normalized T-DC interactions and in vitro proliferation and increased lymph node entry of $G\alpha_{12}$,$G\alpha_{13}$ double-deficient T cells. Also the fact that hyperproliferation is only observed in response to adhesion-dependent stimulation by DCs, but not in response to direct stimulation of the T cell receptor (TCR), PMA, or superantigens, points to the important role of LFA-1 in this context.

The increased adhesiveness observed in the absence of $G\alpha_{12}$ and $G\alpha_{13}$, however, is moderate compared to that observed in a mouse line carrying a hyperactive LFA-1 mutant (*Itgal*$^{\Delta/\Delta}$) containing a five amino acid deletion in the membrane-proximal region of LFA-1 (Semmrich et al., 2005). *Itgal*$^{\Delta/\Delta}$ lymphocytes share with $G\alpha_{12}$,$G\alpha_{13}$ double-deficient cells in vitro phenotypes such as increased ICAM-1 adhesion, impaired transmigration, and tail retraction, but they differ considerably with respect to their in vivo phenotype. In vivo, *Itgal*$^{\Delta/\Delta}$ mice resemble LFA-1-deficient animals, with reduced lymph node and thymus sizes and impaired proliferative responses (Berlin-Rufenach et al., 1999; Schmits et al., 1996). These paradoxical findings are most likely due to the constitutive active nature of the *Itgal*$^{\Delta/\Delta}$ mutant, and this nature leads to irrevocable attachment to HEV or DCs and thereby prevents normal transmigration or activation. In $G\alpha_{12}$,$G\alpha_{13}$ double-deficient T cells, in contrast, negative regulation of LFA-1 through other mechanisms such as cbl-b (Zhang et al., 2003) or RhoH (Cherry et al., 2004) is still functional, leading to the observed moderate changes in trafficking and proliferation.

Our in vitro studies suggest that the inactivation of $G\alpha_{12}$ and $G\alpha_{13}$ results in an altered activation state of three small GTPases involved in the regulation of polarization and integrin-mediated adhesion: RhoA, Rac1, and Rap1. RhoA has been shown to regulate integrin activity in T cells both positively (Constantin et al., 2000; Giagulli et al., 2004) and negatively (Rodriguez-Fernandez et al., 2001; Smith et al., 2003); in addition, it has been involved in polarization (Iden and Collard, 2008; Mor et al., 2007). RhoA is probably the most important effector of $G\alpha_{12}$ and $G\alpha_{13}$, but it should be kept in mind that RhoA can also be activated by a variety of other signaling pathways such as integrins, receptor tyrosine kinases, plexins, or G_q and G_i family G proteins. RhoA activation in response to stimulation of G_{12},G_{13}-coupled receptors is mediated by three specific RhoGEF proteins, Lsc, LARG, and PDZ-RhoGEF (Fukuhara et al., 2001), and our data indicate that Lsc, and to a lesser extent also LARG, mediate the inhibitory effects of $G\alpha_{12}$ and $G\alpha_{13}$ on adhesion and proliferation. In line with these findings, Lsc-deficient mice share some phenotypical aspects with T cell-specific $G\alpha_{12}$,$G\alpha_{13}$ double-deficient mice, for example increased lymph node size and in vitro proliferation (Girkontaite et al., 2001) or impaired rear detachment from ICAM-1 (Rubtsov et al., 2005). An increased polarization was also observed in $G\alpha_{12}$,$G\alpha_{13}$ double-deficient B cells (Rieken et al., 2006b) or in neutrophils expressing dominant-negative forms of $G\alpha_{12}$ and $G\alpha_{13}$ (Xu et al., 2003). Xu et al. (2003) suggested that chemoattractant receptors might activate G_i- and G_{12},G_{13}-mediated signaling pathways in neutrophils in parallel, whereas our data suggest that G_{12},G_{13}-mediated quenching of chemokine-induced Rac1 activity involves receptors other than CCR7, for example, TP.

RhoA is known to antagonistically regulate Rac1, a small GTPase involved in the regulation of cellular morphology, polarization, and integrin signaling (Iden and Collard, 2008; Mor et al., 2007). We found that both basal and chemokine-induced Rac1 activation is increased in the absence of $G\alpha_{12}$ and $G\alpha_{13}$, possibly contributing to enhanced polarization and integrin-mediated adhesion of $G\alpha_{12}$,$G\alpha_{13}$ double-deficient T cells (D'Souza-Schorey et al., 1998; Garcia-Bernal et al., 2005). We furthermore show that chemokine-induced Rac1 activation in control $CD4^+$ T cells is dampened by concomitant simulation of the G_{12},G_{13}-RhoA pathway through the TP agonist U46619. Interestingly,

U46619 alone induces Rac1 activation through G proteins of the G_q family (Gratacap et al., 2001); it seems, however, that during combined application of U46619 and CCL19+21, the G_{12},G_{13}-RhoA mediated inhibition of Rac1 outweighs G_q-induced Rac1 activation. Importantly, stimulation of the G_{12},G_{13}-RhoA signaling cascade by U46619 does not only impede CCL19+21-induced Rac1 activation but also impacts on adhesiveness and, consecutively, on proliferation: U46619 is able to reduce conjugate formation between wild-type $CD4^+$ T cells and allo-DCs, resulting in reduced proliferation in vitro. Of note, the $G\alpha_{12}$,$G\alpha_{13}$-mediated modulation of adhesiveness and proliferation was not restricted to U46619, but was also observed in response to LPA and, to a lesser extent, S1P. We therefore hypothesize that local mediators such as S1P, LPA, and TXA_2 are released from lymphocytes or bystanding cells and modulate cell polarization and integrin-mediated adhesion in an auto- or paracrine manner. Lysophospholipids and TXA_2 are released from blood cells, macrophages, and dendritic cells (Chun and Rosen, 2006; Kabashima et al., 2003) and are therefore likely to contribute to the regulation of cell-cell interactions during lymph node entry or antigen presentation. Genetic inactivation of the TXA_2 receptor TP, for example, resulted in age-dependent lymphadenopathy and enhanced immune responses to foreign antigens (Kabashima et al., 2003). In line with an important role of $G\alpha_{12}$ and $G\alpha_{13}$ in the negative regulation of adhesiveness through auto- and paracrine factors, we found that gentle washing significantly increased ICAM-1 adhesiveness in control but not in $G\alpha_{12}$,$G\alpha_{13}$ double-deficient T cells.

The third GTPase that shows altered activation in the absence of $G\alpha_{12}$ and $G\alpha_{13}$ is Rap1, which has been shown to increase integrin-mediated adhesion (Katagiri et al., 2000; Sebzda et al., 2002), for example in response to chemokine receptor activation (Shimonaka et al., 2003). Whether increased chemokine-induced Rap1 activation in the absence of $G\alpha_{12}$ and $G\alpha_{13}$ is causally related to increased Rac1 and impaired RhoA activation is currently unclear. Crosstalk between Rac1 and Rap1 has been implicated in the regulation of cell migration, for example by localizing GEFs for Rap1 and Rac1 to the ruffling membrane (Arthur et al., 2004; Caloca et al., 2004), but the effects of $G\alpha_{12}$,$G\alpha_{13}$ on Rap1 and Rac1 might also be independent.

A fourth GTPase involved in the regulation of LFA-1 activity in lymphocytes is RhoH (Cherry et al., 2004). In contrast to other small GTPases, RhoH is GTPase deficient and therefore does not undergo the normal activation-inactivation cycle; instead, it was suggested to be regulated on the transcriptional level (Li et al., 2002). We investigated RhoH expression by RT-PCR but did not find altered expression in the absence of $G\alpha_{12}$ and $G\alpha_{13}$ (data not shown), suggesting that altered RhoH expression does not contribute to the phenotype of T cell-specific $G\alpha_{12}$,$G\alpha_{13}$ double-deficient mice.

Interestingly, whereas LFA-1 activity is clearly enhanced in $G\alpha_{12}$,$G\alpha_{13}$ double-deficient $CD4^+$ T cells, the activation state of integrin $\alpha4\beta1$ is not altered, suggesting that these integrins are differentially regulated. A differential regulation of $\alpha4\beta1$ and LFA-1 by small GTPases has been described in a rat monocytic cell line (Honing et al., 2004) and in human T cells (Ghandour et al., 2007); the underlying mechanisms, however, are unknown. It is also currently unclear why $G\alpha_{12}$,$G\alpha_{13}$ deficiency seems to affect $CD4^+$ T cells more prominently than $CD8^+$ T cells. Differences in the expression of G_{12} family G proteins or of G_{12},G_{13}-coupled receptors might explain these findings, but neither in literature (Chun and Rosen, 2006; Kabashima et al., 2003) nor in our own experiments did we find evidence for such differences. It might be speculated that not yet characterized G_{12},G_{13}-coupled receptors with cell type-specific expression are involved in the negative regulation of integrin activity.

The in vivo relevance of the G_{12},G_{13}-mediated negative regulation of LFA-1 is clearly documented by the finding that T cell-specific $G\alpha_{12}$,$G\alpha_{13}$ double-deficient mice show an increased susceptibility toward endogenous and exogenous antigens, resulting in increased severity of autoimmune diabetes and cutaneous hypersensitivity. Interestingly, except for the increased lymph node size, we did not detect signs of spontaneous autoimmune disease in T cell-specific $G\alpha_{12}$,$G\alpha_{13}$ double-deficient mice, suggesting that the regulatory effect of $G\alpha_{12}$ and $G\alpha_{13}$ is especially important under pathological conditions.

Taken together, our data show that heterotrimeric G proteins of the G_{12} family negatively regulate the activation state of integrin LFA-1, thereby fine-tuning T cell trafficking, proliferation, and susceptibility toward immune disease. We show that a variety of receptor systems such as lysophospholipid or prostanoid receptors converge on $G\alpha_{12}$ and $G\alpha_{13}$ to modulate activation of RhoA, Rac1, Rap1, and ultimately LFA-1, and it is well possible that other, yet unknown mediators contribute to this process. Therefore, a cell-type-specific manipulation of $G\alpha_{12}$ and $G\alpha_{13}$ or of downstream RhoGEF proteins might in the future prove useful to modulate T cell trafficking or the strength of the immunological synapse.

EXPERIMENTAL PROCEDURES

Animals and Cells

Mice were housed under specific pathogen-free conditions, and their genetic background was predominantly C57BL6/N (fifth generation backcross). Genotyping was performed as described previously (Moers et al., 2003). For generation of conditional LARG-deficient mice, please see Supplemental Experimental Procedures. Untouched lymph node $CD4^+$ T cells and splenic $CD11c^+$ dendritic cells were isolated with the mouse $CD4^+$ T cell isolation kit or mouse CD11c-Microbeads, respectively (Miltenyi, Bergisch-Gladbach, Germany). All animal experiments have been approved by local authorities.

Chemicals and Antibodies

U46619 was from Cayman (Ann Arbor, MI, USA); LPA and S1P were from Biomol (Hamburg, Germany), chemokines from PeproTech (London, UK); and STZ, DNFB, staphylococcal enterotoxin B, and α-tubulin antibodies were from Sigma-Aldrich (St. Louis, MO, USA). Endotoxin-free antibodies against LFA-1, VLA4, or isotype control were from the Cancer Research UK Monoclonal Antibody Unit, London. Antibodies against $G\alpha_{13}$, $G\alpha_{12}$, and LARG were from Santa Cruz Biotechnology (Santa Cruz, CA, USA). All other antibodies were from BD Biosciences (San Jose, CA, USA).

Flow Cytometry

All flow cytometric analyses were performed with a FACSCalibur flow cytometer and CellQuestPro Software (BD Biosciences). Apoptosis and proliferation were determined with the Annexin-V-FITC apoptosis kit and the FITC-BrdU flow kit, respectively; intracellular cytokine production was determined with the mouse intracellular cytokine staining kit (all BD Biosciences). For the flow cytometric analysis of conjugate formation, 1×10^5 PE-labeled $CD4^+$ T cells and 1×10^5 FITC-labeled $CD11c^+$ DCs were mixed, centrifuged for 1 min at 50 × g, and incubated for 20 min. After gentle resuspension, the proportion of CFSE-PE double-positive events was determined.

Live-Cell Imaging

For live-cell imaging, 10^5 unstained purified $CD4^+$ T cells from control or mutant mice were mixed with 2 $\times 10^4$ CFSE-labeled $CD11c^+$ DCs in a droplet of 20 μl RPMI1640, 10 mM HEPES, and 10% FCS and allowed to attach to CELL STAR plastic dishes (Greiner Bio-One GmbH, Essen, Germany) for 20 min at 37°C and 5% CO_2. In some cases, 10 μg/ml LFA-1 antibodies, 10 μg/ml α4β1 antibodies, or 10 μg/ml isotype control were added to the mixture. Cell interactions were recorded for 10 min with a Leica DM IRE2 inverted fluorescence microscope and Leica FW4000 software at 37°C and 5% CO_2 (1 frame per 10 s). For statistical analysis, cell interactions were classified by an investigator blinded to genotype; an interaction was classified as stable if it lasted throughout a 10 min movie. In some cases, plates were coated with ICAM-1 (for coating, see Adhesion Assays) and the distance traveled by individual T cells was determined with the ImageJ program (NIH, Bethesda, MD, USA).

Adhesion Assays

Adhesion assays were carried out in 48-well plastic dishes as described previously (Rieken et al., 2006a), with minor modifications: for ICAM-1 coating, wells were coated with 50 μg/ml goat-anti-human-IgG-Fc antibody (Jackson ImmunoResearch, West Grove, PA, USA) at 4°C overnight, washed twice with PBS, and incubated with 2.5 μg/ml mouse ICAM-1-F_c (R&D Systems, Minneapolis, USA) in PBS for 2 hr. For VCAM-1 coating, wells were incubated for 1 hr at 37°C with 3 μg/ml hVCAM-1 (R&D Systems) in carbonate buffer. In some cases, chemokines CCL19 and 21 were added at final concentrations of 100 ng/ml during ICAM-1 and hVCAM-1 coating. Afterward, all wells were blocked with 0.5% bovine serum albumine (BSA) in PBS for 30 min before use. The volume per well was 100 μl in each step. For the adhesion assay, 5 × 10^5 lymph node cells were incubated in 100 μl RPMI1640 containing 10 mM HEPES and 0.5% FCS for 30 min at 37°C and 5% CO_2; in some cases, CCL19 and CCL21 (100 ng/ml final), Mg^{2+} (10 mM) and EGTA (1 mM), CD3-CD28 antibodies (5 μg/ml each), or PMA (5 ng/ml) were added. After discarding nonadherent cells, the plate was gently washed in PBS and adherent cells were subsequently detached in RPMI1640, 5 mM EDTA for 20 min on ice. Numbers of adherent $CD4^+$ T cells were determined after antibody staining by flow cytometry, and data are displayed as the proportion of adherent cells relative to cell input into the adhesion assay.

Soluble ICAM-1 Binding

Binding of ICAM-1 (10 μg/ml, R&D Systems) to $CD4^+$ T cells in the absence or presence of 10 mM Mg^{2+} and 1 mM EGTA was determined as described previously (Sebzda et al., 2002). In brief, freshly isolated lymph node cells (1 × 10^5 cells/ml) were resuspended in HEPES buffer (20 mM HEPES, 140 mM NaCl, and 2 g/l glucose) with 0.1% BSA at a concentration of 2 × 10^6 cells/ml. Lymphocyte aliquots of 50 μl (1 × 10^5 cells) were added to 96-well plates with or without 10 mM Mg^{2+} and 1 mM EGTA. Soluble murine ICAM-1–Fc (10 μg/ml, R&D Systems) was added to the cells. After 30 min incubation at 37°C, cells were washed twice in ice-cold PBS with 0.1% BSA and incubated with Fc-specific FITC-conjugated goat anti-human IgG (1:200; Jackson Immunoresearch, West Grove, PA, USA) and PerCP-conjugated anti-mouse CD4 antibody for 10 min on ice. We washed cells twice in PBS with 0.1% BSA to remove excess unbound antibodies and detected fluorescence by flow cytometry.

Migration Assays

For chemotaxis assays, lymph node cells were preincubated in RPMI1640 + 10 mM HEPES + 0.1% BSA for 30 min at 37°C and 5% CO_2 and then allowed to migrate through 5 μm pore size transwell inserts (Corning, Acton, MA, USA) at a density of 2 × 10^6 splenocytes/100 μl per well. The transwell inserts were uncoated, ICAM-1-coated (as described for Adhesion Assays), or seeded with 3 × 10^4 bEND.3 endothelial cells (from ATCC [Montesano et al., 1990]) 24 hr before the experiment. The lower wells contained either 600 μl RPMI1640 + 10 mM HEPES + 0.1% BSA alone or medium plus 100 ng/ml CCL19+21, or 1–100 nM S1P. After 3 hr of incubation at 37°C and 5% CO_2, transwell plates were kept on ice for 20 min and centrifuged at 180 × g for 3 min, inserts were discarded, and cells were stained for $CD4^+$ T cells and counted by flow cytometry. Cell numbers were expressed as a proportion of input. All experiments were done in triplicates.

Adoptive Transfer Experiments

Fluorescent labeling of cells with the Cell Trace CFSE Cell Proliferation Kit (50 νM CFSE final), CellTracker CM-DiI (5 mM final), or SNARF (500 nM final) (all Invitrogen, Karlsruhe, Germany) was performed according to the manufacturer's instructions. For adoptive transfer experiments, isolated $CD4^+$ T cells from mutant and control animals were labeled with CFSE and DiI, or SNARF, mixed in a 1:1 ratio, and injected intravenously (5 × 10^6 cells per mouse). In some cases, recipients were pretreated with 100 μg LFA-1 antibodies or isotype control. After 2 or 24 hr, the proportion of CFSE- and DiI-positive cells in cervical lymph nodes was analyzed by flow cytometry; in some cases we also analyzed cisterna chyli punctate. All data were corrected for the actual input ratio as determined by FACS.

RhoA, Rac1, and Rap1 Activation Assays

Amounts of GTP-bound RhoA or Rac1 were determined with RhoA or Rac1 G-LISA activation kits (Cytoskeleton, Denver, CO, USA), and Rap1 was detected with the EZ-Detect Rap1 activation kit (Pierce, Rockford, USA). For each measurement, 2 × 10^6 (RhoA) or 5 × 10^6 (Rac1, Rap1) T cells were used; in some cases, cells were pretreated with PTX 100 ng/ml. Agonist concentrations were 1 μM for U46618 and 100 ng/ml for chemokines.

Intravital Two-Photon Microscopy

Three-dimensional two-photon microscopy was performed with a MaiTai laser (Spectra-Physics, Darmstadt, Germany) running at 800 nm, a multibeam scanhead (LaVision Biotech, Bielefeld, Germany), and an Olympus BX51WI microscopic stage equipped with a XLUMPL ×20, NA 0.95 water dipping lens. Image detection was done with a cooled CCD-camera (Imager Intense, LaVision, Goettingen, Germany). RGB Z stacks of 300 × 300 μm images were recorded in typically 15 steps of 3 μm. Frames taken at two to three positions within each of the two imaging areas (vessel-rich zone [medulla, paracortex] and T cell zone) were analyzed (Sanna et al., 2006). Rendering of video sequences was performed with Volocity 4.3 (Improvision, Waltham, MA, USA). Cell tracking was done with computer-assisted manual tracking with CellTracker. Data were plotted with Prism 4 (GraphPad Software, San Diego, CA, USA). Swapping of dyes resulted in the same findings. For details, see Supplemental Experimental Procedures.

Animal Models

Delayed type hypersensitivity and MLD-STZ diabetes mellitus were induced in female (DTH) or male (MLD-STZ) mice aged 8–16 weeks as described previously (Kurimoto and Streilein, 1993; Like and Rossini, 1976). Urine glucose levels were determined with the glucose hexokinase method (Randox Laboratories, UK). For the flow cytometric quantification of pancreatic leukocyte infiltration, the peripancreatic lymph nodes were carefully removed; then pancreata were minced and digested for 10–15 min at 37°C under vigorous shaking in Krebs-Ringer solution containing 0.5 mg/ml Collagenase P (Roche Diagnostics, Mannheim, Germany). Leukocytes were then purified via Percoll and Lympholyte M gradients (Cedarlane, Burlington, Canada) according to the manufacturer's instructions and analyzed by flow cytometry.

In Vitro Proliferation Assays, Immunoblotting, and Immunohistochemistry

In vitro proliferation assays, immunoblotting, and immunohistochemistry were performed as described previously (Rieken et al., 2006a; Rieken et al., 2006b). For details, see Supplemental Experimental Procedures.

Statistics

Data are displayed as mean ± SEM. Comparisons between two groups were performed with unpaired t test. n indicates the number of animals per experimental group.

SUPPLEMENTAL DATA

Supplemental Data include Supplemental Experimental Procedures, one table, three figures, and four movies and can be found with this article online at http://www.cell.com/immunity/supplemental/S1074-7613(09)00183-6.

ACKNOWLEDGMENTS

We thank M. Bernhard, M. Hillesheim, and Y. Teschner for expert technical assistance; J. Marth for the LckCre line; and B. Arnold, R. Arnold, and B. Schraven for helpful advice. This work was funded by the collaborative research center 405 of the *Deutsche Forschungsgemeinschaft* and the *Young Investigator Award* of the Medical Faculty of the University of Heidelberg.

Received: July 8, 2008
Revised: January 9, 2009
Accepted: February 23, 2009
Published online: April 30, 2009

REFERENCES

Arthur, W.T., Quilliam, L.A., and Cooper, J.A. (2004). Rap1 promotes cell spreading by localizing Rac guanine nucleotide exchange factors. J. Cell Biol. *167*, 111–122.

Berlin-Rufenach, C., Otto, F., Mathies, M., Westermann, J., Owen, M.J., Hamann, A., and Hogg, N. (1999). Lymphocyte migration in lymphocyte function-associated antigen (LFA)-1-deficient mice. J. Exp. Med. *189*, 1467–1478.

Caloca, M.J., Zugaza, J.L., Vicente-Manzanares, M., Sanchez-Madrid, F., and Bustelo, X.R. (2004). F-actin-dependent translocation of the Rap1 GDP/GTP exchange factor RasGRP2. J. Biol. Chem. *279*, 20435–20446.

Cherry, L.K., Li, X., Schwab, P., Lim, B., and Klickstein, L.B. (2004). RhoH is required to maintain the integrin LFA-1 in a nonadhesive state on lymphocytes. Nat. Immunol. *5*, 961–967.

Chun, J., and Rosen, H. (2006). Lysophospholipid receptors as potential drug targets in tissue transplantation and autoimmune diseases. Curr. Pharm. Des. *12*, 161–171.

Constantin, G., Majeed, M., Giagulli, C., Piccio, L., Kim, J.Y., Butcher, E.C., and Laudanna, C. (2000). Chemokines trigger immediate beta2 integrin affinity and mobility changes: Differential regulation and roles in lymphocyte arrest under flow. Immunity *13*, 759–769.

D'Souza-Schorey, C., Boettner, B., and Van Aelst, L. (1998). Rac regulates integrin-mediated spreading and increased adhesion of T lymphocytes. Mol. Cell. Biol. *18*, 3936–3946.

Fukuhara, S., Chikumi, H., and Gutkind, J.S. (2001). RGS-containing RhoGEFs: The missing link between transforming G proteins and Rho? Oncogene *20*, 1661–1668.

Garcia-Bernal, D., Wright, N., Sotillo-Mallo, E., Nombela-Arrieta, C., Stein, J.V., Bustelo, X.R., and Teixido, J. (2005). Vav1 and Rac control chemokine-promoted T lymphocyte adhesion mediated by the integrin alpha4beta1. Mol. Biol. Cell *16*, 3223–3235.

Ghandour, H., Cullere, X., Alvarez, A., Luscinskas, F.W., and Mayadas, T.N. (2007). Essential role for Rap1 GTPase and its guanine exchange factor CalDAG-GEFI in LFA-1 but not VLA-4 integrin mediated human T-cell adhesion. Blood *110*, 3682–3690.

Giagulli, C., Scarpini, E., Ottoboni, L., Narumiya, S., Butcher, E.C., Constantin, G., and Laudanna, C. (2004). RhoA and zeta PKC control distinct modalities of LFA-1 activation by chemokines: Critical role of LFA-1 affinity triggering in lymphocyte in vivo homing. Immunity *20*, 25–35.

Girkontaite, I., Missy, K., Sakk, V., Harenberg, A., Tedford, K., Potzel, T., Pfeffer, K., and Fischer, K.D. (2001). Lsc is required for marginal zone B cells, regulation of lymphocyte motility and immune responses. Nat. Immunol. *2*, 855–862.

Gratacap, M.P., Payrastre, B., Nieswandt, B., and Offermanns, S. (2001). Differential regulation of Rho and Rac through heterotrimeric G-proteins and cyclic nucleotides. J. Biol. Chem. *276*, 47906–47913.

Gu, J.L., Muller, S., Mancino, V., Offermanns, S., and Simon, M.I. (2002). Interaction of G alpha(12) with G alpha(13) and G alpha(q) signaling pathways. Proc. Natl. Acad. Sci. USA *99*, 9352–9357.

Hennet, T., Hagen, F.K., Tabak, L.A., and Marth, J.D. (1995). T-cell-specific deletion of a polypeptide N-acetylgalactosaminyl-transferase gene by site-directed recombination. Proc. Natl. Acad. Sci. USA *92*, 12070–12074.

Hogg, N., Henderson, R., Leitinger, B., McDowall, A., Porter, J., and Stanley, P. (2002). Mechanisms contributing to the activity of integrins on leukocytes. Immunol. Rev. *186*, 164–171.

Honing, H., van den Berg, T.K., van der Pol, S.M., Dijkstra, C.D., van der Kammen, R.A., Collard, J.G., and de Vries, H.E. (2004). RhoA activation promotes transendothelial migration of monocytes via ROCK. J. Leukoc. Biol. *75*, 523–528.

Iden, S., and Collard, J.G. (2008). Crosstalk between small GTPases and polarity proteins in cell polarization. Nat. Rev. Mol. Cell Biol. *9*, 846–859.

Kabashima, K., Murata, T., Tanaka, H., Matsuoka, T., Sakata, D., Yoshida, N., Katagiri, K., Kinashi, T., Tanaka, T., Miyasaka, M., et al. (2003). Thromboxane A2 modulates interaction of dendritic cells and T cells and regulates acquired immunity. Nat. Immunol. *4*, 694–701.

Katagiri, K., Hattori, M., Minato, N., Irie, S., Takatsu, K., and Kinashi, T. (2000). Rap1 is a potent activation signal for leukocyte function-associated antigen 1 distinct from protein kinase C and phosphatidylinositol-3-OH kinase. Mol. Cell. Biol. *20*, 1956–1969.

Kim, M., Carman, C.V., Yang, W., Salas, A., and Springer, T.A. (2004). The primacy of affinity over clustering in regulation of adhesiveness of the integrin {alpha}L{beta}2. J. Cell Biol. *167*, 1241–1253.

Kinashi, T. (2005). Intracellular signalling controlling integrin activation in lymphocytes. Nat. Rev. Immunol. *5*, 546–559.

Kurimoto, I., and Streilein, J.W. (1993). Studies of contact hypersensitivity induction in mice with optimal sensitizing doses of hapten. J. Invest. Dermatol. *101*, 132–136.

Laudanna, C., and Alon, R. (2006). Right on the spot. Chemokine triggering of integrin-mediated arrest of rolling leukocytes. Thromb. Haemost. *95*, 5–11.

Laudanna, C., Kim, J.Y., Constantin, G., and Butcher, E. (2002). Rapid leukocyte integrin activation by chemokines. Immunol. Rev. *186*, 37–46.

Li, X., Bu, X., Lu, B., Avraham, H., Flavell, R.A., and Lim, B. (2002). The hematopoiesis-specific GTP-binding protein RhoH is GTPase deficient and modulates activities of other Rho GTPases by an inhibitory function. Mol. Cell. Biol. *22*, 1158–1171.

Like, A.A., and Rossini, A.A. (1976). Streptozotocin-induced pancreatic insulitis: New model of diabetes mellitus. Science *193*, 415–417.

Matloubian, M., Lo, C.G., Cinamon, G., Lesneski, M.J., Xu, Y., Brinkmann, V., Allende, M.L., Proia, R.L., and Cyster, J.G. (2004). Lymphocyte egress from thymus and peripheral lymphoid organs is dependent on S1P receptor 1. Nature *427*, 355–360.

Matsuoka, T., and Narumiya, S. (2007). Prostaglandin receptor signaling in disease. ScientificWorldJournal *7*, 1329–1347.

Moers, A., Nieswandt, B., Massberg, S., Wettschureck, N., Gruner, S., Konrad, I., Schulte, V., Aktas, B., Gratacap, M.P., Simon, M.I., et al. (2003). G13 is an essential mediator of platelet activation in hemostasis and thrombosis. Nat. Med. *9*, 1418–1422.

Montesano, R., Pepper, M.S., Mohle-Steinlein, U., Risau, W., Wagner, E.F., and Orci, L. (1990). Increased proteolytic activity is responsible for the aberrant morphogenetic behavior of endothelial cells expressing the middle T oncogene. Cell *62*, 435–445.

Mor, A., Dustin, M.L., and Philips, M.R. (2007). Small GTPases and LFA-1 reciprocally modulate adhesion and signaling. Immunol. Rev. *218*, 114–125.

Offermanns, S., Mancino, V., Revel, J.P., and Simon, M.I. (1997). Vascular system defects and impaired cell chemokinesis as a result of Galpha13 deficiency. Science *275*, 533–536.

Rieken, S., Herroeder, S., Sassmann, A., Wallenwein, B., Moers, A., Offermanns, S., and Wettschureck, N. (2006a). Lysophospholipids control integrin-dependent adhesion in splenic B cells through G(i) and G(12)/G(13) family G-proteins but not through G(q)/G(11). J. Biol. Chem. *281*, 36985–36992.

Rieken, S., Sassmann, A., Herroeder, S., Wallenwein, B., Moers, A., Offermanns, S., and Wettschureck, N. (2006b). G12/G13 family G proteins regulate marginal zone B cell maturation, migration, and polarization. J. Immunol. *177*, 2985–2993.

Riobo, N.A., and Manning, D.R. (2005). Receptors coupled to heterotrimeric G proteins of the G12 family. Trends Pharmacol. Sci. *26*, 146–154.

Rodriguez-Fernandez, J.L., Sanchez-Martin, L., Rey, M., Vicente-Manzanares, M., Narumiya, S., Teixido, J., Sanchez-Madrid, F., and Cabanas, C. (2001). Rho and Rho-associated kinase modulate the tyrosine kinase PYK2 in T-cells through regulation of the activity of the integrin LFA-1. J. Biol. Chem. *276*, 40518–40527.

Rubtsov, A., Strauch, P., Digiacomo, A., Hu, J., Pelanda, R., and Torres, R.M. (2005). Lsc regulates marginal-zone B cell migration and adhesion and is required for the IgM T-dependent antibody response. Immunity *23*, 527–538.

Sanna, M.G., Wang, S.K., Gonzalez-Cabrera, P.J., Don, A., Marsolais, D., Matheu, M.P., Wei, S.H., Parker, I., Jo, E., Cheng, W.C., et al. (2006). Enhancement of capillary leakage and restoration of lymphocyte egress by a chiral S1P1 antagonist in vivo. Nat. Chem. Biol. *2*, 434–441.

Schmits, R., Kundig, T.M., Baker, D.M., Shumaker, G., Simard, J.J., Duncan, G., Wakeham, A., Shahinian, A., van der Heiden, A., Bachmann, M.F., et al. (1996). LFA-1-deficient mice show normal CTL responses to virus but fail to reject immunogenic tumor. J. Exp. Med. *183*, 1415–1426.

Sebzda, E., Bracke, M., Tugal, T., Hogg, N., and Cantrell, D.A. (2002). Rap1A positively regulates T cells via integrin activation rather than inhibiting lymphocyte signaling. Nat. Immunol. *3*, 251–258.

Semmrich, M., Smith, A., Feterowski, C., Beer, S., Engelhardt, B., Busch, D.H., Bartsch, B., Laschinger, M., Hogg, N., Pfeffer, K., and Holzmann, B. (2005). Importance of integrin LFA-1 deactivation for the generation of immune responses. J. Exp. Med. *201*, 1987–1998.

Shimaoka, M., Takagi, J., and Springer, T.A. (2002). Conformational regulation of integrin structure and function. Annu. Rev. Biophys. Biomol. Struct. *31*, 485–516.

Shimonaka, M., Katagiri, K., Nakayama, T., Fujita, N., Tsuruo, T., Yoshie, O., and Kinashi, T. (2003). Rap1 translates chemokine signals to integrin activation, cell polarization, and motility across vascular endothelium under flow. J. Cell Biol. *161*, 417–427.

Smith, A., Bracke, M., Leitinger, B., Porter, J.C., and Hogg, N. (2003). LFA-1-induced T cell migration on ICAM-1 involves regulation of MLCK-mediated attachment and ROCK-dependent detachment. J. Cell Sci. *116*, 3123–3133.

Smith, A., Stanley, P., Jones, K., Svensson, L., McDowall, A., and Hogg, N. (2007). The role of the integrin LFA-1 in T-lymphocyte migration. Immunol. Rev. *218*, 135–146.

van Kooyk, Y., van Vliet, S.J., and Figdor, C.G. (1999). The actin cytoskeleton regulates LFA-1 ligand binding through avidity rather than affinity changes. J. Biol. Chem. *274*, 26869–26877.

Xu, J., Wang, F., Van Keymeulen, A., Herzmark, P., Straight, A., Kelly, K., Takuwa, Y., Sugimoto, N., Mitchison, T., and Bourne, H.R. (2003). Divergent signals and cytoskeletal assemblies regulate self-organizing polarity in neutrophils. Cell *114*, 201–214.

Zhang, W., Shao, Y., Fang, D., Huang, J., Jeon, M.S., and Liu, Y.C. (2003). Negative regulation of T cell antigen receptor-mediated Crk-L-C3G signaling and cell adhesion by Cbl-b. J. Biol. Chem. *278*, 23978–23983.